

# Tree-Embedded Bayesian Factor Models for Multidimensional Categorical Distributions

Naoki Awaya<sup>\*1</sup>, Keisuke Sasaki<sup>\*2</sup>, Genya Kobayashi<sup>3</sup> and Shonosuke Sugasawa<sup>4</sup>

<sup>1</sup>*School of Political Science and Economics, Waseda University*

<sup>2</sup>*Graduate School of Economics, The University of Tokyo*

<sup>3</sup>*School of Commerce, Meiji University*

<sup>4</sup>*Department of Economics, Keio University*

\*These authors contributed equally to this work.

## Abstract

Analyzing data collected from multiple sources to estimate common and heterogeneous structures through a hierarchical model is a central task in Bayesian inference, and to this end, Bayesian factor models are one of the most widely used tools for this purpose. In this paper, we propose a new Bayesian latent factor model for distributions, providing a parsimonious model for describing many observed distributions through lower-dimensional structures. Many applications are found in the social science in the form of grouped data, for example, distributions of age composition and income observed across locations. In these contexts, standard mixture models can be inefficient because the distributions do not necessarily exhibit clear clustering structures. To overcome the difficulty, we introduce a tree-based transformation that embeds distributions into a Euclidean space and construct a Bayesian latent factor model in the transformed space. Once transformed into Euclidean vectors, the Bayesian hierarchical model can be extended in a straightforward manner. As an illustration, we incorporate spatial dependence by introducing a prior based on a simultaneous autoregressive (SAR) model. The proposed model is “nonparametric” in the sense that it does not impose parametric assumptions on the form of the observed distributions. Through numerical experiments using real population data, we demonstrate that the proposed model outperforms the standard Dirichlet mixture model as well as models built on parametric assumptions.

## 1 Introduction

There are many datasets in which each observational unit is itself a probability distribution rather than a single scalar or vector. A motivating example arises in population studies, where each location is characterized by an empirical distribution describing the demographic composition of residents across age and gender categories. Similar distribution-valued observations appear in other settings in the social science, such as income distributions across regions or grouped responses in large-scale

surveys. In these contexts, the primary research interest is not in estimating each distribution separately, but in understanding how distributions vary across units and whether such variation can be summarized through a lower-dimensional structure. Developing statistical tools that extract such common structure while respecting the intrinsic constraints of probability distributions is therefore of central importance.

To combine information across multiple samples while maintaining interpretability, a natural approach is to employ Bayesian factor models. In this framework, a large number of observed distributions can be explained through a substantially smaller number of latent factors. For example, in population data, although hundreds of distributions may be observed across locations, they may be driven by only a few latent characteristics, such as the ratios of population in the young/working age/elderly categories. Bayesian factor models are well-suited to such settings because they automatically identify the factors that account for major differences among observations. However, applying factor models directly to distributional data is not straightforward, since standard formulations assume observations lie in Euclidean space rather than on a probability simplex.

To bridge the gap between distributional data and the standard Bayesian toolbox, we propose to transform distributions using a binary tree partition structure, generalizing the ideas proposed in the biostatistical analysis with the phylogenetic and taxonomic tree (Wang et al., 2021). As formulated in Wang et al. (2021) through the “logistic-tree” construction, a bijection can be established between a distribution and a set of conditional probabilities defined on the internal nodes of a tree. Applying a logistic transformation yields a Euclidean vector representation while preserving the one-to-one relationship with the original distribution.

An important advantage of adopting a tree-based representation is that it naturally preserves the ordering structure of categories, allowing nearby values to belong to the same node or to share common ancestors in the tree. This property is particularly useful for grouped or continuous data, where adjacent categories are expected to behave similarly. Furthermore, the proposed framework avoids parametric assumptions about the underlying distributional process. Tree-based models for unsupervised analysis have been studied in nonparametric Bayesian inference, most notably through the Pólya tree process (Lavine, 1992; Hanson, 2006; Wong and Ma, 2010), which enables flexible estimation of distributions. In the proposed framework, we parameterize distributions through a similar tree-based construction. Consequently, the proposed model can flexibly describe distributions that deviate from parametric assumptions, as demonstrated in the numerical evaluation in Section 3.

Another advantage of employing a tree-based decomposition is that the framework extends naturally to multidimensional settings, as also demonstrated in analyses based on the Pólya tree process (Wong and Ma, 2010; Awaya and Ma, 2024). Given a tree-partition structure, multidimensional distributions can be represented through essentially the same recursive construction used for univariate distributions (an example of such a tree is illustrated in Figure 3). This property is particularly useful in social science applications, where datasets often involve multiple variables, such as population data with joint age–gender compositions or survey data consisting of multiple questionnaire items.

One may wonder why a new Bayesian factor model is needed instead of relying on mixture-based approaches such as Dirichlet mixture models or Dirichlet process mixtures. In many social science applications, distributional data do not exhibit clear clustering structures; rather, distributions often change gradually across locations or other characteristics, and, as shown in Section 3, mixture models tend to produce an excessively large number of clusters in such settings. When clustering structure is weak or absent, factor models provide a more parsimonious representation, describing diverse distributions through a small number of latent factors. As an illustration, Figure 2 visualizes simulated distributions generated from the proposed factor model with only two factors (details are provided in Section 2), demonstrating that the simplex can be densely covered. This contrasts sharply with mixture-based representations: as illustrated in Figure 2, a mixture model with two components can only trace an essentially one-dimensional trajectory between the components.

We note that the proposed tree-based decomposition is not the only way to map distributions into Euclidean space. For example, several types of transformations have been proposed in the context of compositional data analysis (see, e.g., Aitchison, 1982; Egozcue et al., 2003; Silverman et al., 2017). However, as discussed in Wang et al. (2024) and Section 2, the tree representation facilitates Bayesian modeling with computationally convenient Gibbs samplers enabled by Polya–Gamma augmentation (Polson et al., 2013).

Once each distribution is represented as a Euclidean vector, extending the Bayesian hierarchical model becomes straightforward. As a demonstration, we incorporate a simultaneous autoregressive (SAR) prior on factor loadings to capture spatial dependence across locations. We further introduce the infinite factor model (Bhattacharya and Dunson, 2011), together with post-processing procedures proposed in Aßmann et al. (2016) and De Vito et al. (2021), to automatically calibrate the effective number of factors. We note that these components represent only one possible realization within the proposed framework; alternative Bayesian factor models or additional covariate structures could be incorporated in a similar manner.

In the remainder of the paper, Section 2 introduces a new factor modeling framework for categorical data based on a novel tree-based decomposition of distributions. We incorporate spatial correlation to illustrate the flexibility of the framework, although the proposed model can accommodate other types of hierarchical structures as well. Section 3 presents an application to stay-population data collected in an urban area of Japan, together with an empirical comparison against alternative models for categorical data. Section 4 concludes the article.

## 2 Tree-Embedded Factor Models for Categorical Distributions

### 2.1 Logistic-tree decomposition of grouped data

In this section, we describe a tree-based decomposition of grouped data, which serves as the foundation for the proposed factor model and its spatial extension.

Let  $\Omega$  denote the collection of all finite categories under consideration. The elements of  $\Omega$  may

be indexed by multiple features; for example, in population data each category may correspond to a specific combination of gender and age group. We assume that a dyadic tree-partition structure  $T$  is constructed over the categories in  $\Omega$ . An illustrative example is provided in Figure 3, where the tree is defined for two-dimensional categories. In some settings a natural tree structure is available (e.g., phylogenetic trees for microbiome data (Wang et al., 2021)), whereas in many applications it is necessary to construct a data-adaptive tree. Details of tree construction are provided in Section 2.6.

The tree  $T$  induces a collection of leaf (external) nodes and internal nodes, denoted by  $\mathcal{L}(T)$  and  $\mathcal{N}(T)$ , respectively. To denote the nodes of the tree, we adopt the recursive expression following the literature on the Pólya tree process (Soriano and Ma, 2017; Awaya and Ma, 2024); A generic node in the tree is denoted by  $A$ , and if  $A \in \mathcal{N}(T)$ , it is partitioned into two child nodes, denoted by  $A_l$  and  $A_r$ . We let the number of internal nodes be denoted by  $N$ , resulting in  $N + 1$  categories in total.

Suppose  $P$  is a discrete distribution defined on the categories in  $\Omega$ . Throughout the discussion, we focus on the collection of discrete distributions with positive masses, namely,

$$\mathcal{P}_{N+1} = \left\{ (p_1, \dots, p_{N+1}) : p_1 \in (0, 1), \dots, p_{N+1} \in (0, 1), \sum_{l=1}^{N+1} p_l = 1 \right\}.$$

A key property of distributions defined along a tree partition is that, as shown in the literature on the Pólya tree process (e.g., (Lavine, 1992; Hanson, 2006)), the distribution is uniquely characterized by conditional probabilities defined on the internal nodes:

$$\theta(A) := P(A_l | A), \quad A \in \mathcal{N}(T).$$

Hence, posterior inference for the distribution reduces to estimating the parameters  $\theta$ . Figure 1 illustrates a tree with two layers and three internal nodes ( $A$ ,  $A_l$ , and  $A_r$ ), where a discrete distribution with four masses ( $p_1, p_2, p_3, p_4$ ) is parameterized by  $\theta(A)$ ,  $\theta(A_l)$ , and  $\theta(A_r)$ .

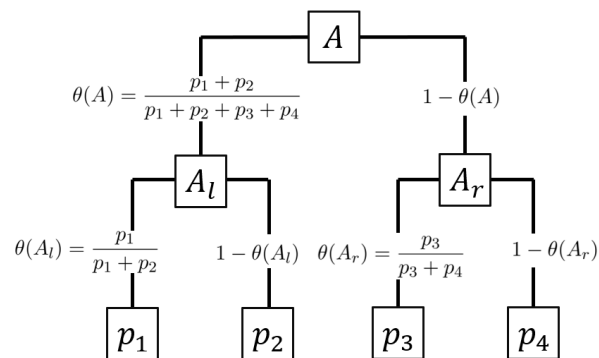


Figure 1: Illustration of a two-layer tree with three internal-node parameters.

Because the likelihood for each  $\theta(A)$  takes a binomial form based on counts within  $A_l$  and  $A_r$ , many Pólya tree models adopt beta priors for conjugacy (Ma and Wong, 2011; Soriano and Ma, 2017;

Awaya and Ma, 2024). In this work, however, we follow the logistic-tree normal formulation (Jara and Hanson, 2011; Wang et al., 2021) and introduce logit-transformed parameters

$$\psi(A) := \log\left(\frac{\theta(A)}{1 - \theta(A)}\right).$$

This transformation defines a bijection between the original parameters  $\{\theta(A)\}_{A \in \mathcal{N}(T)} \subset [0, 1]^N$  and the transformed parameters  $\{\psi(A)\}_{A \in \mathcal{N}(T)} \subset \mathbb{R}^N$ . Equivalently, we define a tree-based embedding  $\mathcal{E}_T : \mathcal{P}_{N+1} \rightarrow \mathbb{R}^N$  by

$$\mathcal{E}_T(P) = \{\psi(A)\}_{A \in \mathcal{N}(T)}.$$

The transformed representation is particularly convenient for hierarchical modeling because the support becomes unconstrained, enabling Gaussian-based modeling strategies. The hierarchical model with the Gaussian process prior is formulated in Jara and Hanson (2011), and Wang et al. (2021) demonstrate richer latent structures through graphical-lasso-type priors and mixture models. Building on this structure, we introduce a novel factor model for distributional observations.

## 2.2 Factor models for discrete distributions

We introduce a new factor model that represents a collection of distributions through a smaller number of latent factor distributions. Suppose that we observe  $M$  distributions defined on the category set  $\Omega$ . For  $i = 1, \dots, M$ , let  $n_i(B)$  denote the number of observations falling in a subset  $B \subset \Omega$ . We assume that the counts  $n_i$  are generated from an unknown distribution  $P_i$ , and, using the tree-based embedding  $\mathcal{E}_T$ , we define

$$\{\psi_i(A)\}_{A \in \mathcal{N}(T)} = \mathcal{E}_T(P_i).$$

For notational convenience, we denote the parameter vector  $\{\psi_i(A)\}_{A \in \mathcal{N}(T)}$  by  $\psi_i$ .

The central idea of factor analysis is to explain high-dimensional observations, here the  $M$  distributions, through a lower-dimensional structure characterized by  $K$  latent factors. Since the unknown distributions are mapped into a Euclidean space, we can adopt the standard formulation of Bayesian factor models (Lopes and West, 2004; Prado and West, 2010). Let  $\boldsymbol{\eta}_1, \dots, \boldsymbol{\eta}_K$  be  $N$ -dimensional vectors, which we interpret as factor distributions. Because the tree-logit transformation is bijective, each  $\boldsymbol{\eta}_k$  implicitly corresponds to a set of conditional probabilities on the tree  $T$ , and hence to a discrete distribution on  $\Omega$ . We model each embedded vector  $\psi_i$  as

$$\psi_i = \lambda_{i1}\boldsymbol{\eta}_1 + \dots + \lambda_{iK}\boldsymbol{\eta}_K, \tag{1}$$

where  $\lambda_{i1}, \dots, \lambda_{iK} \in \mathbb{R}$  are scalar factor loadings. Under this formulation, the model combines the  $K$  distributions

$$\mathcal{E}_T^{-1}(\boldsymbol{\eta}_1), \dots, \mathcal{E}_T^{-1}(\boldsymbol{\eta}_K)$$

within the Euclidean embedding space. More generally, we can introduce a mean vector  $\boldsymbol{\mu} = \{\mu(A)\}_{A \in \mathcal{N}(T)}$  and write

$$\psi_i = \boldsymbol{\mu} + \lambda_{i1}\boldsymbol{\eta}_1 + \dots + \lambda_{iK}\boldsymbol{\eta}_K. \tag{2}$$

The mean  $\boldsymbol{\mu}$  can be fixed to reflect prior structural information, for example based on the number of categories associated with each node, or treated as an unknown parameter. Our preliminary experiments suggest that estimating  $\boldsymbol{\mu}$  jointly with the factor components may introduce weak identifiability between  $\boldsymbol{\mu}$  and the latent factors.

An immediate, but important property of the proposed model is that the intrinsic dimension of the induced space of distributions equals the number of factors  $K$ , which sharply contrasts with standard mixture models. To illustrate this difference, consider a three-dimensional simplex and two distributions

$$d_1 = (1/3, 1/3, 1/3), \quad d_2 = (1/2, 1/3, 1/6).$$

Under a typical mixture model, the  $i$ th distribution is expressed as

$$w_i d_1 + (1 - w_i) d_2,$$

where  $w_i$  denotes the mixture weight. In contrast, the proposed factor model represents distributions via the Euclidean embedding

$$\lambda_{i1} \mathcal{E}_T(d_1) + \lambda_{i2} \mathcal{E}_T(d_2).$$

Figure 2 presents ternary plots of 200 simulated distributions (simulation details are provided in Appendix B). By construction, the mixture model generates points along a one-dimensional curve connecting the two components. In contrast, the logistic-tree factor model can represent a substantially richer family of distributions across the simplex; in theory, any distribution in the simplex can be approximated through suitable factor coefficients. This expressive power is obtained because the loadings  $\lambda_{i1}$  and  $\lambda_{i2}$  are unconstrained real values rather than restricted to  $(0, 1)$ . For instance, for the component  $d_2$ , the coefficient  $\lambda_{i2}$  may exceed 1 or be negative, allowing the model to represent both distributions concentrated on the first dimension and those emphasizing the second and third dimensions.

### 2.3 Prior specification based on the infinite factor model

To provide a discussion on the prior specification, it is convenient to express the factor model in a nodewise form for each internal node  $A \in \mathcal{N}(T)$ . An equivalent representation of (2) is given by

$$\boldsymbol{\psi}(A) = \boldsymbol{\mu}(A) \boldsymbol{\iota}_M + \mathbf{\Lambda} \boldsymbol{\eta}(A), \tag{3}$$

where  $\boldsymbol{\iota}_M$  denotes the  $M \times 1$  vector of ones, and

$$\boldsymbol{\psi}(A) = \begin{bmatrix} \psi_1(A) \\ \vdots \\ \psi_M(A) \end{bmatrix}, \quad \boldsymbol{\eta}(A) = \begin{bmatrix} \eta_1(A) \\ \vdots \\ \eta_K(A) \end{bmatrix},$$

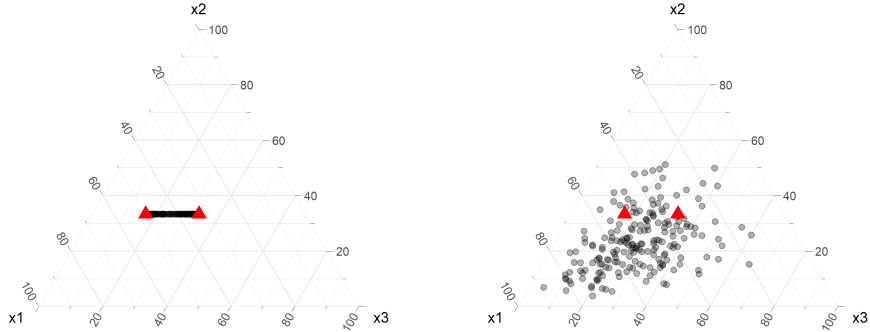


Figure 2: Illustration of simulated distributions generated from a two-component mixture model (left) and the proposed factor model (right). Red triangles indicate the component distributions.

and  $\mathbf{\Lambda}$  is the  $M \times K$  loading matrix

$$\mathbf{\Lambda} = \begin{bmatrix} \lambda_{11} & \lambda_{12} & \cdots & \lambda_{1K} \\ \lambda_{21} & \lambda_{22} & \cdots & \lambda_{2K} \\ \vdots & \vdots & \ddots & \vdots \\ \lambda_{M1} & \lambda_{M2} & \cdots & \lambda_{MK} \end{bmatrix}.$$

Careful prior specification for  $\mathbf{\Lambda}$  is essential, since factors and loadings are not identifiable under rotations and switching signs. A common strategy is to impose structural constraints on the loading matrix, for example by setting upper-triangular entries  $\lambda_{ik}$  ( $i < k$ ) to zero (Geweke and Zhou, 1996; Aguilar and West, 2000). Such approaches, however, require a pre-specified ordering of observations and may substantially affect posterior inference. Instead, we adopt the infinite factor model of Bhattacharya and Dunson (2011) together with the post-processing procedure of De Vito et al. (2021), which avoids ordering constraints and enables data-driven selection of the effective number of factors.

In many applications, additional structural information is available and should be incorporated through the prior. For example, in population data the spatial locations of observations are known, and it is desirable to borrow strength across nearby regions. To achieve this, we introduce a simultaneous autoregressive (SAR) prior for the loading vectors based on an adjacency matrix  $W$ , whose rows are normalized to sum to one. Although we focus on the SAR specification, the proposed framework is compatible with alternative spatial priors, such as the CAR model considered in Wakayama and Sugasawa (2024).

Within the infinite factor framework (Bhattacharya and Dunson, 2011), the prior on loadings is designed so that their scales decrease with the factor index. We therefore choose an initial truncation level  $K$  moderately large (e.g.,  $K = 10$ ) in order to provide a good approximation to the correlation structure. Based on this framework, for the  $k$ th column of the loadings matrix  $\mathbf{\Lambda}_{\cdot k}$ , we introduce

a combination of the sparsity inducing prior from Bhattacharya and Dunson (2011) and the SAR model; Let  $\rho_k \in (-1, 1)$  be the correlation parameter and  $W$  be the adjacency matrix. Then, we introduce the prior that is induced by the following model:

$$(I_M - \rho_k W) \mathbf{\Lambda}_{\cdot k} \sim N(\mathbf{0}, (\tau_k \Phi_k)^{-1}),$$

where  $\Phi_k = \text{diag}(\phi_{1,k}, \dots, \phi_{M,k})$  introduces local shrinkage with

$$\phi_{i,k} \sim \text{Gamma}\left(\frac{\nu}{2}, \frac{\nu}{2}\right), \quad i = 1, \dots, M,$$

and  $\tau_k$  is the global precision parameter following the multiplicative gamma process (Bhattacharya and Dunson, 2011):

$$\tau_k = \prod_{l=1}^k \delta_l, \quad \delta_1 \sim \text{Gamma}(a_1, 1), \quad \delta_l \sim \text{Gamma}(a_2, 1) \quad (l \geq 2).$$

In this prior, the difference  $\mathbf{\Lambda}_{\cdot k} - \rho_k W \mathbf{\Lambda}_{\cdot k}$  represents residual variation not explained by neighboring locations, to which sparsity-inducing shrinkage is applied. The precision matrix of the Gaussian distribution that the loading vector  $\mathbf{\Lambda}_{\cdot k}$  follows is

$$\tau_k (I_M - \rho_k W^T) \Phi_k (I_M - \rho_k W),$$

which implies decreasing variance across factor indices due to the multiplicative gamma prior on  $\tau_k$ . For the correlation parameter  $\rho_k$ , we adopt a truncated normal prior  $\text{TN}_{(-1,1)}(m_\rho, s_\rho^2)$ .

Following Durante (2017) and De Vito et al. (2021), we set  $(a_1, a_2) = (2.1, 3.1)$  and  $\nu = 3$ . For  $\rho_k$ , we specify a weakly informative prior by choosing  $(m_\rho, s_\rho^2)$  accordingly.

## 2.4 Posterior sampling

Deriving the posterior sampling algorithm is straightforward because, as discussed in Wang et al. (2024), the logistic-tree formulation allows the introduction of Pólya–Gamma (PG) augmentation (Polson et al., 2013). We briefly outline the PG augmentation for the proposed model here, while detailed sampling steps are provided in Appendix A.

For location  $i$  ( $i = 1, \dots, M$ ) and an internal node  $A \in \mathcal{N}(T)$ , the likelihood of observing  $n_i(A_l)$  counts in  $A_l$  out of  $n_i(A)$  total observations follows the binomial distribution and can be written as

$$\begin{aligned} p(n_i(A_l) \mid n_i(A), \psi_i(A)) &= \left( \frac{\exp(\psi_i(A))}{1 + \exp(\psi_i(A))} \right)^{n_i(A_l)} \left( \frac{1}{1 + \exp(\psi_i(A))} \right)^{n_i(A_r)} \\ &= \frac{\exp(\psi_i(A))^{n_i(A_l)}}{\{1 + \exp(\psi_i(A))\}^{n_i(A)}}. \end{aligned}$$

Following Polson et al. (2013), this likelihood admits a Pólya–Gamma mixture representation:

$$\begin{aligned} &p(n_i(A_l) \mid n_i(A), \psi_i(A)) \\ &\propto \exp(\kappa_i(A) \psi_i(A)) \int_0^\infty \exp\left\{-\frac{\omega_i(A) \psi_i(A)^2}{2}\right\} p(\omega_i(A) \mid n_i(A), 0) d\omega_i(A), \end{aligned}$$

where  $\kappa_i(A) = n_i(A_I) - n_i(A)/2$  and  $\omega_i(A) \sim \text{PG}(n_i(A), 0)$ .

Based on the augmentation, the model admits a pseudo-linear Gaussian representation. To describe it, we define the  $M \times 1$  vector  $\boldsymbol{\kappa}(A)$  and the diagonal matrix  $\boldsymbol{\Omega}(A)$  by

$$\boldsymbol{\kappa}(A) = \begin{bmatrix} \kappa_1(A) \\ \kappa_2(A) \\ \vdots \\ \kappa_M(A) \end{bmatrix}, \quad \boldsymbol{\Omega}(A) = \begin{bmatrix} \omega_1(A) & 0 & \cdots & 0 \\ 0 & \omega_2(A) & & \vdots \\ \vdots & & \ddots & 0 \\ 0 & \cdots & 0 & \omega_M(A) \end{bmatrix}.$$

Also,  $\boldsymbol{\iota}_M$  denotes the  $M \times 1$  vector filled with 1, namely,  $(1, \dots, 1)^T$ .

Then, given  $\boldsymbol{\Omega}(A)$ , the likelihood for the parameters related to the internal node  $A$  can be written as the pseudo-regression model

$$\boldsymbol{\Omega}(A)^{-1}\boldsymbol{\kappa}(A) = \mu(A)\boldsymbol{\iota}_M + \mathbf{\Lambda}\boldsymbol{\eta}(A) + \boldsymbol{\epsilon}(A), \quad (4)$$

where  $\boldsymbol{\epsilon}(A) \sim N(\mathbf{0}, \boldsymbol{\Omega}(A)^{-1})$  is an auxiliary Gaussian noise term. Hence, conditional on the latent variables  $\boldsymbol{\Omega}(A)$ , the likelihood reduces to a Gaussian linear model with pseudo-observation  $\boldsymbol{\Omega}(A)^{-1}\boldsymbol{\kappa}(A)$ . The resulting MCMC sampling algorithm follows from standard Gaussian models and is summarized in Appendix A.

## 2.5 Post-processing for the factor loadings

The infinite factor model employed in this work has strong expressive power for capturing the correlation structure among the  $M$  observed distributions. For interpretability, however, it is necessary to determine the number of factors that effectively explain the dependence structure. In addition, the prior on the loading matrix does not impose constraints that resolve the non-identifiability problem arising from sign switching and rotational invariance (see, e.g., Papastamoulis and Ntzoufras, 2022). To address these issues, we adopt the post-processing strategy of De Vito et al. (2021).

### 2.5.1 Selecting the optimal number of factors

As implied by the model formulations in (3) and (4), and noting that the factors  $\boldsymbol{\eta}(A)$  follow standard Gaussian priors, the dominant component governing the correlation among the  $M$  distributions is  $\mathbf{\Lambda}\mathbf{\Lambda}^\top$ , a symmetric positive semi-definite matrix of rank  $K$ . When  $\mathbf{\Lambda}$  is given, the effective dimensionality of the factor representation can be assessed through the ordered eigenvalues, analogously to the analysis based on scree plots: Following De Vito et al. (2021), we determine the effective number of factors  $K^*$  as follows. First, at each MCMC iteration we compute the ordered eigenvalues of  $\mathbf{\Lambda}\mathbf{\Lambda}^\top$  and estimate their posterior means. Second, based on the cumulative proportion of explained variation, we select  $K^*$  as the smallest index for which the cumulative contribution exceeds a pre-specified threshold (e.g., 90%).

### 2.5.2 Addressing the identifiability problem

After determining the effective number of factors  $K^*$  ( $K^* < K$ ), we need to transform the posterior samples of the loading matrix from  $M \times K$  to  $M \times K^*$  representations while preserving the essential structure of the inferred factors and resolving rotational ambiguity.

To describe the post-processing procedure, we let  $\{\mathbf{\Lambda}^{(r)}\}_{r=1}^R$  denote posterior draws of the loading matrix. We consider transformations of the form  $\mathbf{\Lambda}^{(r)}\mathbf{Q}^{(r)}$ , where  $\mathbf{Q}^{(r)}$  has orthonormal columns satisfying  $(\mathbf{Q}^{(r)})^\top \mathbf{Q}^{(r)} = I_{K^*}$ . The collection  $\{\mathbf{Q}^{(r)}\}_{r=1}^R$  is chosen to minimize a loss relative to a reference loading matrix  $\mathbf{\Lambda}^*$ . Specifically, following Aßmann et al. (2016) and Papastamoulis and Ntzoufras (2022), we minimize

$$\frac{1}{R} \sum_{r=1}^R \text{tr} \left\{ (\mathbf{\Lambda}^{(r)}\mathbf{Q}^{(r)} - \mathbf{\Lambda}^*)^\top (\mathbf{\Lambda}^{(r)}\mathbf{Q}^{(r)} - \mathbf{\Lambda}^*) \right\},$$

where one minimizes the Frobenius norm averaged with respect to the posterior.

The numerical solutions are obtained using the iterative algorithm introduced in Aßmann et al. (2016). Because the solution is not unique and depends on initial values, we follow their recommendation and initialize the procedure using the posterior sample.

### 2.6 Tree construction based on the Aitchison geometry

In many application scenarios, a tree structure suitable for the logistic-tree decomposition is not available a priori, and therefore an automated tree-construction procedure is required. Note that several computational methods have been proposed to estimate an appropriate tree for estimating distributional structures (e.g., Ram and Gray, 2011; Wong and Ma, 2010; Awaya and Ma, 2020). However, our primary goal in the factor analysis is not density estimation itself but estimating the structure in the variability among the observed distributions. In other words, we seek a tree on which the difference among the distributions is most clarified.

To achieve this, we adopt the principal balances algorithm (Glahn et al., 2011), which constructs tree structures based on isometric log-ratio (ilr) coordinates (See Egozcue et al., 2003, for details). Within the ilr framework, an orthonormal basis is defined through a binary tree partition. For each internal node  $A$  split into  $A_l$  and  $A_r$ , a given distribution yields a coordinate known as a “balance”,

$$\sqrt{\frac{|A_l||A_r|}{|A_l| + |A_r|}} \log \frac{g(A_l)}{g(A_r)},$$

where  $|A_l|$  and  $|A_r|$  denote the numbers of categories in the respective nodes, and  $g(A_l)$  and  $g(A_r)$  represent the geometric means of probabilities within each subset. The variability of balances across observed distributions quantifies how strongly a given partition captures differences among distributions, conceptually analogous to variance explained by rotated coordinates in the principal component analysis.

We employ the maximum explained variance hierarchical balances (MV) algorithm of Glahn et al. (2011), which follows a coarse-to-fine greedy strategy. When splitting a node  $A$ , candidate partitions are evaluated by computing the variance of the resulting balances, and the split maximizing this variance is selected. While the original MV algorithm evaluates only a subset of candidate splits, the relatively small number of categories in our applications allows us to exhaustively evaluate all possible partitions.

As an illustration, Figure 3 displays the tree constructed from the population data observed at 19:00 on 12/24/2019. The two-dimensional categories are first divided into gender-based groups, indicating that variation among locations is primarily driven by the female-to-male composition. Within each gender category, subsequent splits highlight differences associated with older age groups (e.g., individuals aged 60 or above).

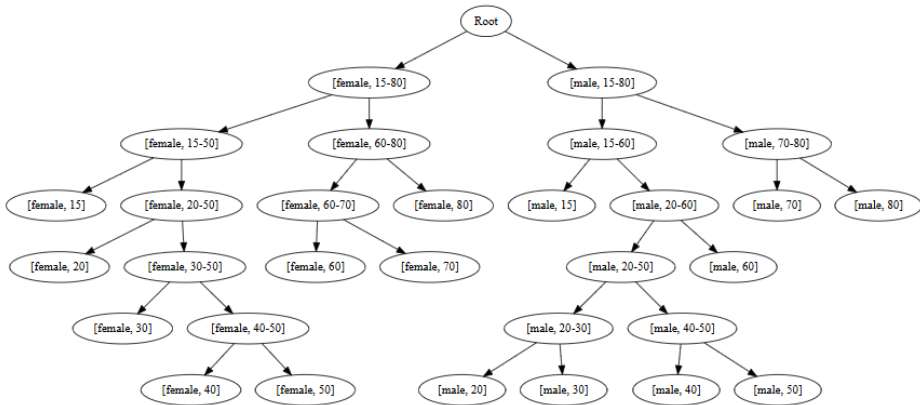


Figure 3: Visualization of the tree partition obtained using the MV algorithm for the population data observed at 19:00 on 12/24/2019.

### 3 Application to the Spatial Population Data

In this empirical study, we analyze the stay-population data provided by NTT Docomo, one of the largest mobile carriers in Japan with more than 90 million accounts. Based on their operational data, the number of mobile terminals in each base station area is counted. Then, the population of each area is extrapolated with high accuracy using the penetration rate of NTT Docomo (see Terada et al. (2013); Oyabu et al. (2013)). We consider the 500 meter mesh data over the five special wards of Tokyo (Figure 4), including  $M = 452$  observation locations. A sample of the observed distributions is also illustrated in Figure 4. The same data set has been used in different Bayesian contexts of spatial or spatiotemporal analysis (see, for example, Wakayama and Sugawara, 2024; Wakayama et al., 2025).

In contrast to the previous studies above, which only considered populations of gender-age-total, in this analysis, we consider the distributions of population by gender and age. Specifically, the

dataset provides two gender categories (Male and Female) and eight age groups: 15–19, 20–29, 30–39, 40–49, 50–59, 60–69, 70–79, and 80 years or older. Consequently, for each location and time point, the observation is represented as a frequency vector with  $N + 1 = 16$  categories. In this analysis, we extract specific time points from February, July, and December 2019 and independently analyze data for the selected time points.

We begin with a quantitative comparison with existing models designed to analyze compositional data, based on the Posterior Predictive Loss (PPL) defined in Gelfand and Ghosh (1998). We then summarize the main findings obtained with the proposed factor model.

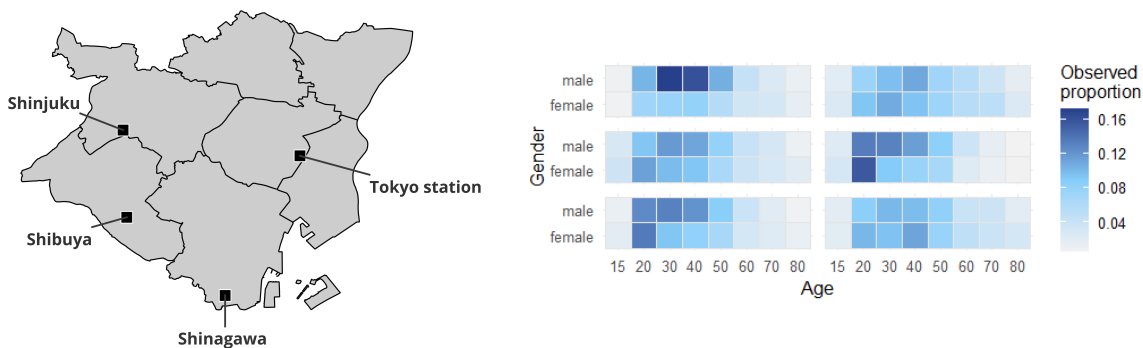


Figure 4: Left: Map of the districts where the spatiotemporal population data were collected. The four locations that are discussed in the application results are indicated. Right: Observed distributions in six randomly selected locations at 19:00 on 12/24/2019.

### 3.1 Numerical comparison

We compare the proposed model with two existing approaches for compositional data that rely on different modeling strategies. The first model is the Dirichlet process mixture model (DPM), where each mixture component is the multinomial distribution. This model is one of the most standard nonparametric models for estimating discrete distributions and is capable of adequately capturing a clustering structure in the data if it exists. The second model is the Log-normal model with the pairwise difference prior (Log-normal PWD) proposed in Sugasawa et al. (2020) for analyzing grouped data with spatial correlation. They model each observed distribution using a discretized version of a parametric distribution and for the parameters in the different locations, by introducing a prior incorporating the spatial correlation with the  $L_2$ -type loss for adjacent locations. An essential difference from our proposed model is that the parametric assumption is crucial. Although we report results based on the Log-normal specification, our preliminary experiments show that a similar tendency is observed under different specifications for the observed distributions. The details of these competing methods are provided in Appendix B.

The primary evaluation metric for comparing the three models is the Posterior Predictive Loss

(PPL) defined in (Gelfand and Ghosh, 1998), where smaller values indicate a better trade-off between model fit and model complexity. Adapting their original formulation to the specific structure of the population data, we define the PPL for a given model  $\mathcal{M}$  as

$$\text{PPL}(\mathcal{M}) = \frac{1}{M} \sum_{i=1}^M \sum_{j=1}^{N+1} V_{ij}^{\mathcal{M}} + \frac{1}{M+1} \sum_{i=1}^M \sum_{j=1}^{N+1} (y_{ij}^{obs} - E_{ij}^{\mathcal{M}})^2,$$

where  $y_{ij}^{obs}$  represents the observed count for the  $j$ -th category at the  $i$ -th location, and  $E_{ij}^{\mathcal{M}}$  and  $V_{ij}^{\mathcal{M}}$  denote the mean and variance of the posterior predictive distribution under model  $\mathcal{M}$ , respectively.

For the proposed factor model and the DPM models, the PPL is calculated by fitting the data to the full 16 distinct categories comprising eight age groups and two genders. For the proposed model specifically, the reported PPL is calculated after selecting the optimal number of factors,  $K^*$ , which is chosen as the smallest index where the cumulative proportion of explained variation exceeds 95%. In contrast, the Log-normal PWD model is applied separately to each gender, and the reported PPL in Table 1 represents the sum of these gender-specific PPLs. This approach is necessary because the Log-normal PWD model works for categories with an ordinal structure and cannot accommodate the full 16-category structure directly, as gender is a nominal variable without a natural ordering. Table 1 reports the PPL values for all models across the nine selected time points. These points were selected to cover a diverse range of day types, such as weekdays, weekends, and holidays, as well as various times of day, including early morning, daytime, evening, and late night. The results show that the proposed factor model achieves substantially lower PPL values than the two benchmark models at every time point.

Table 1: Posterior predictive loss (PPL) for Proposed model, DPM, and Log-normal PWD evaluated at various temporal contexts.

| Time Point                             | PPL by Model   |           |                |
|--|----------------|-----------|----------------|
|  | Proposed model | DPM       | Log-normal PWD |
| Feb 11 (Mon) 12:00 (National Holiday)  | 7,729.41       | 18,557.88 | 176,363.01     |
| Feb 17 (Sun) 16:00 (Weekend Afternoon) | 7,947.97       | 17,868.61 | 291,714.42     |
| Feb 20 (Wed) 14:00 (Weekday Midday)    | 14,253.07      | 34,153.10 | 601,891.99     |
| Jul 1 (Mon) 09:00 (Weekday Morning)    | 12,726.74      | 32,432.46 | 522,508.83     |
| Jul 20 (Sat) 16:00 (Weekend Afternoon) | 8,835.10       | 20,889.83 | 349,866.24     |
| Jul 25 (Thu) 23:00 (Weekday Night)     | 5,954.42       | 14,944.88 | 78,609.38      |
| Dec 11 (Wed) 05:00 (Early Morning)     | 5,366.60       | 13,346.57 | 60,839.18      |
| Dec 24 (Tue) 19:00 (Christmas Eve)     | 9,825.14       | 24,241.71 | 521,854.54     |
| Dec 31 (Tue) 18:00 (New Year’s Eve)    | 5,174.62       | 12,300.21 | 116,541.54     |

To better understand the performance gap relative to the DPM model, Table 2 presents the posterior summary statistics for the number of clusters obtained by fitting the DPM model at three

representative time points. We observe that the number of clusters is excessively large at all time points, suggesting that the population data do not exhibit a clear clustering structure.

Table 2: Posterior mean and 95% credible intervals of the number of clusters in the DPM Model

| Time Point         | Lower | Mean   | Upper |
|--------------------|-------|--------|-------|
| Feb 11 (Mon) 12:00 | 104   | 106.42 | 109   |
| Jul 1 (Mon) 09:00  | 135   | 138.67 | 142   |
| Dec 31 (Tue) 18:00 | 66    | 68.03  | 70    |

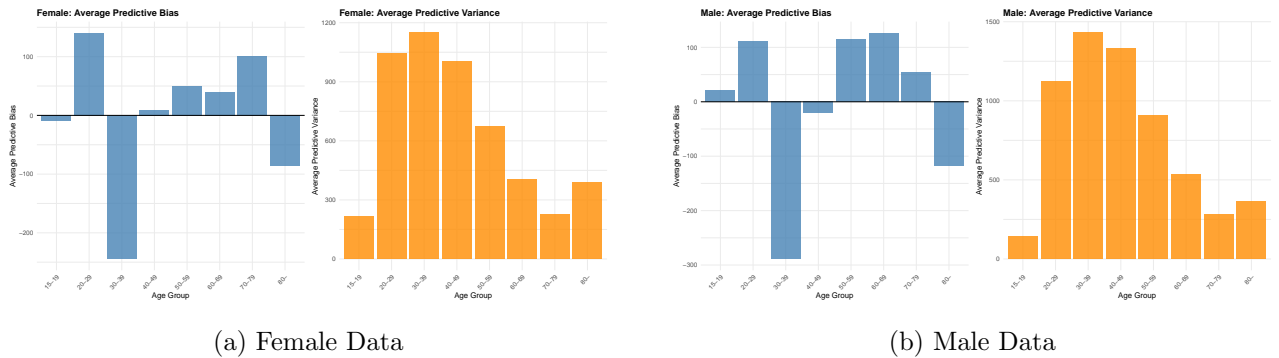


Figure 5: Decomposition of PPL components for the Log-normal PWD model by gender. Panels (a) and (b) display the results for female and male data, respectively. In each panel, the left chart shows the average predictive bias, and the right chart in each panel displays the average predictive variance.

We next examine the behavior of the Log-normal PWD model. Figure 5 illustrates the decomposition of the Posterior Predictive Loss (PPL) for the Log-normal PWD model based on the data collected at 14:00 on February 20, with results categorized by gender in Figures 5a and 5b. In each panel, the left chart displays the average predictive bias, defined as the mean difference between the observed population counts and the posterior predictive means:

$$\frac{1}{M} \sum_{i=1}^M (y_{ij}^{obs} - E_{ij}^{\mathcal{M}}), \quad j = 1, \dots, N + 1.$$

Accordingly, positive values indicate underestimation by the model, while negative values represent overestimation. The right chart illustrates the average predictive variance, expressed as

$$\frac{1}{M} \sum_{i=1}^M V_{ij}^{\mathcal{M}}, \quad j = 1, \dots, N + 1,$$

which quantifies the magnitude of predictive uncertainty.

Closer inspection of these plots highlights a fundamental limitation of the Log-normal PWD model. For both genders, the bias plots reveal a distinct structural trend rather than random fluctuation around zero. The estimation transitions from underestimation in the 20s to peak overestimation in the 30s, reverts to underestimation between the 50s and 70s, and shifts back to overestimation from the 80s onward. Correspondingly, the predictive variance exhibits a consistent cross-gender pattern. It is notably larger among young-to-middle working-age populations, peaking in the 30-39 age group. Together, these complex trajectories in both bias and variance confirm that applying a simple unimodal parametric distribution is insufficient to accurately capture the true shape of the observed population data.

In summary, this comparative analysis highlights the advantages of the proposed factor model for analyzing spatial population data. While the DPM model struggled to identify a parsimonious cluster structure and the Log-normal PWD model exhibited both systematic biases and significant predictive variance due to its parametric assumption, the proposed factor model consistently achieved the lowest PPL values across diverse temporal contexts. These results underscore the proposed method’s capability to effectively capture complex, heterogeneous dependency structures that standard parametric or clustering-based approaches fail to resolve.

### 3.2 Summary of the distributional factor analysis

We next describe a detailed analysis of the results obtained with the proposed factor model, focusing on the specific time and date at 19:00 on December 24th. We use the tree structure  $T$  visualized in Figure 3 to transform the count data into Euclidean vectors. The number of factors selected in the post-processing is  $K^* = 4$ .

For each factor index  $k$  ( $k = 1, \dots, K^*$ ), one natural way to interpret the estimated factor is to show the posterior of the distributions defined by

$$\mu(A) + c_k \eta_k(A), \quad \mu(A) - c_k \eta_k(A), \quad A \in \mathcal{N}(T),$$

where  $c_k > 0$  controls the magnitude of deviation along the  $k$ th factor direction. In our analysis, we set  $c_k$  to the standard deviation of the estimated factor loadings across the  $M$  locations multiplied by two. These two representative distributions illustrate how population compositions vary across locations with positive versus negative loadings.

The resulting typical distributions along with the estimated factor loadings are shown in Figure 6, and we can see that the dominant structure of the data is primarily captured by the first two factors. For instance, distributions associated with positive loadings in the first factor ( $k = 1$ ) place higher probability mass on males aged 20–40, a demographic strongly associated with full-time employment. The corresponding loading map aligns well with geographic characteristics of Tokyo: locations with positive loadings (red regions) include major business districts and transportation hubs such as Tokyo Station and Shinagawa Station. The result for the second factor is also well interpretable: the typical distribution with negative loadings mainly consists of younger age groups (20–30), and the locations

with negative loadings (blue regions) cover major commercial and entertainment areas, including Shibuya and Shinjuku.

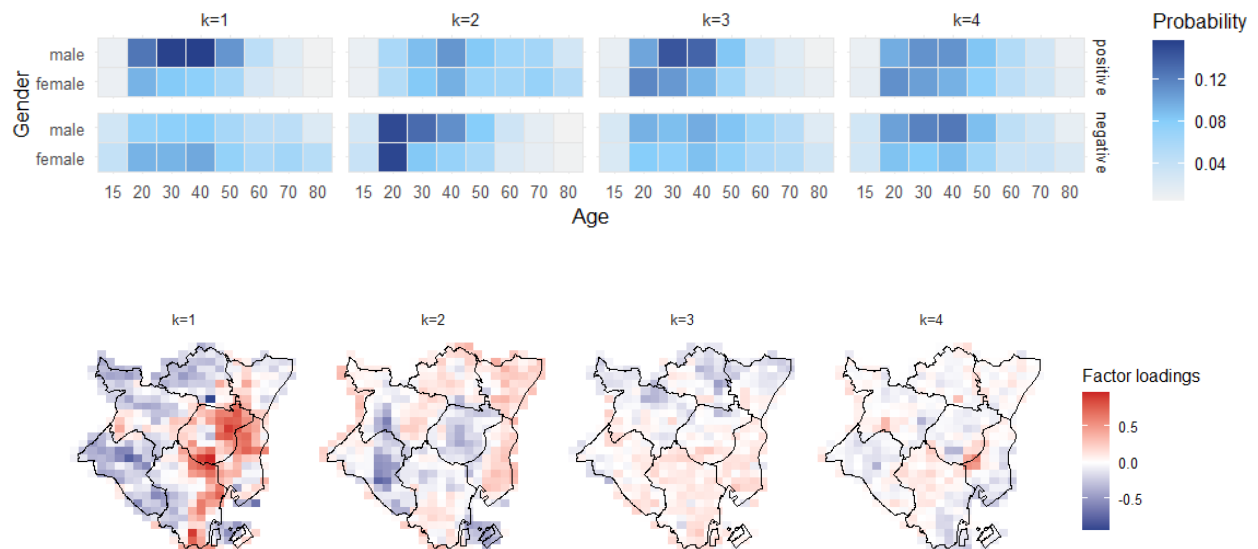


Figure 6: A visualization of the analysis of the population data (19:00 on 12/24/2019) using the proposed distributional factor model. Top: the typical distributions for each factor with positive/negative factor loadings. Bottom: The estimated factor loadings shown on the map.

## 4 Discussion

In this paper, we proposed a Bayesian distributional factor modeling framework that integrates tree-based representations of grouped data with infinite factor models to capture complex variability among multiple observed distributions through lower-dimensional latent factors. By embedding discrete distributions into Euclidean space via a logistic-tree transformation, the proposed approach enables flexible hierarchical modeling, as illustrated through the incorporation of a spatial SAR prior. The tree-based nonparametric representation allows diverse distributional shapes to be captured, while posterior computation remains tractable through Pólya  $\gamma$ -Gamma augmentation. More broadly, the proposed framework provides a bridge between compositional data analysis and modern Bayesian factor modeling.

Through an empirical analysis of spatiotemporal population data in Tokyo, we demonstrated that the proposed method yields a parsimonious yet expressive characterization of heterogeneous demographic patterns, outperforming clustering-based and parametric alternatives in predictive performance. These findings highlight the advantages of factor-based representations for distributional data exhibiting continuous variation rather than clearly separated cluster structures.

An important direction for future work is to extend the proposed framework to explicitly build a spatio-temporal dynamic model. For example, in the context of population data, such an extension could capture temporal pattern of distributions within a day or across seasons, and enable sequential prediction of counts for specific gender–age categories at each location.

## 5 Acknowledgements

This work is partially supported by Japan Society for Promotion of Science (KAKENHI) grant number 24K00244, 25H00546, 25K16618, and 24H00142.

## References

- Omar Aguilar and Mike West. Bayesian dynamic factor models and portfolio allocation. *Journal of Business & Economic Statistics*, 18(3):338–357, 2000.
- John Aitchison. The statistical analysis of compositional data. *Journal of the Royal Statistical Society: Series B (Methodological)*, 44(2):139–160, 1982.
- Christian Aßmann, Jens Boysen-Hogrefe, and Markus Pape. Bayesian analysis of static and dynamic factor models: An ex-post approach towards the rotation problem. *Journal of Econometrics*, 192(1):190–206, 2016.
- Naoki Awaya and Li Ma. Hidden markov Pólya trees for high-dimensional distributions. *arXiv preprint arXiv:2011.03121*, 2020.
- Naoki Awaya and Li Ma. Hidden markov pólya trees for high-dimensional distributions. *Journal of the American Statistical Association*, 119(545):189–201, 2024.
- Anirban Bhattacharya and David B Dunson. Sparse bayesian infinite factor models. *Biometrika*, 98(2):291–306, 2011.
- Roberta De Vito, Ruggero Bellio, Lorenzo Trippa, and Giovanni Parmigiani. Bayesian multistudy factor analysis for high-throughput biological data. *The annals of applied statistics*, 15(4):1723–1741, 2021.
- Daniele Durante. A note on the multiplicative gamma process. *Statistics & Probability Letters*, 122:198–204, 2017.
- Juan José Egozcue, Vera Pawlowsky-Glahn, Glòria Mateu-Figueras, and Carles Barcelo-Vidal. Isometric logratio transformations for compositional data analysis. *Mathematical geology*, 35(3):279–300, 2003.

- M. D. Escobar and M West. Bayesian density estimation and inference using mixtures. *Journal of the American Statistical Association*, 90(430):577–588, 1995.
- A. E. Gelfand and S. K. Ghosh. Model choice: a minimum posterior predictive loss approach. *Biometrika*, 85:1—11, 1998.
- John Geweke and Guofu Zhou. Measuring the pricing error of the arbitrage pricing theory. *The review of financial studies*, 9(2):557–587, 1996.
- Pawlowsky Glahn, Vera, Egozcue Rubí, Juan José, and Raimon Tolosana Delgado. Principal balances. In *Proceedings of the 4th International Workshop on Compositional Data Analysis (2011)*, pages 1–10. International Centre for Numerical Methods in Engineering (CIMNE), 2011.
- Timothy E Hanson. Inference for mixtures of finite polya tree models. *Journal of the American Statistical Association*, 101(476):1548–1565, 2006.
- Alejandro Jara and Timothy E Hanson. A class of mixtures of dependent tail-free processes. *Biometrika*, 98(3):553–566, 2011.
- Michael Lavine. Some aspects of Pólya tree distributions for statistical modelling. *The Annals of Statistics*, 20(3):1222–1235, 1992.
- Hedibert Freitas Lopes and Mike West. Bayesian model assessment in factor analysis. *Statistica Sinica*, pages 41–67, 2004.
- Li Ma and Wing Hung Wong. Coupling optional pólya trees and the two sample problem. *Journal of the American Statistical Association*, 106(496):1553–1565, 2011.
- R. M. Neal. Markov chain sampling methods for dirichlet process mixture models. *Journal of computational and graphical statistics*, 9(2):249–265, 2000.
- Yuki Oyabu, Masayuki Terada, Takayasu Yamaguchi, Shunya Iwasawa, Junichiro Hagiwara, and Daisuke Koizumi. Evaluating reliability of mobile spatial statistics. *NTT DOCOMO Technical Journal*, 14(3):16–23, 2013.
- Panagiotis Papastamoulis and Ioannis Ntzoufras. On the identifiability of bayesian factor analytic models. *Statistics and Computing*, 32(2):23, 2022.
- Nicholas G Polson, James G Scott, and Jesse Windle. Bayesian inference for logistic models using pólya–gamma latent variables. *Journal of the American statistical Association*, 108(504):1339–1349, 2013.
- Raquel Prado and Mike West. *Time series: modeling, computation, and inference*. Chapman and Hall/CRC, 2010.

- Parikshit Ram and Alexander G Gray. Density estimation trees. In *Proceedings of the 17th ACM SIGKDD international conference on Knowledge discovery and data mining*, pages 627–635, 2011.
- Justin D Silverman, Alex D Washburne, Sayan Mukherjee, and Lawrence A David. A phylogenetic transform enhances analysis of compositional microbiota data. *elife*, 6:e21887, 2017.
- Jacopo Soriano and Li Ma. Probabilistic multi-resolution scanning for two-sample differences. *Journal of the Royal Statistical Society: Series B (Statistical Methodology)*, 79(2):547–572, 2017.
- Shonosuke Sugasawa, Genya Kobayashi, and Yuki Kawakubo. Estimation and inference for area-wise spatial income distributions from grouped data. *Computational Statistics & Data Analysis*, 145:106904, 2020.
- Masayuki Terada, Tomohiro Nagata, and Motonari Kobayashi. Population estimation technology for mobile spatial statistics. *NTT DOCOMO Technical Journal*, 14(3):10–15, 2013.
- Tomoya Wakayama and Shonosuke Sugasawa. Spatiotemporal factor models for functional data with application to population map forecast. *Spatial Statistics*, 62:100849, 2024.
- Tomoya Wakayama, Shonosuke Sugasawa, and Genya Kobayashi. Similarity-based random partition distribution for clustering functional data. *Journal of the Royal Statistical Society Series C: Applied Statistics*, 75(1):100–119, 06 2025. ISSN 0035-9254. doi: 10.1093/jrsssc/qlaf037. URL <https://doi.org/10.1093/jrsssc/qlaf037>.
- Zhuoqun Wang, Jialiang Mao, and Li Ma. Microbiome compositional analysis with logistic-tree normal models. *arXiv preprint arXiv:2106.15051*, 2021.
- Zhuoqun Wang, Naoki Awaya, and Li Ma. Generative modeling of density regression through tree flows. *arXiv preprint arXiv:2406.05260*, 2024.
- Wing H Wong and Ma. Optional Pólya tree and Bayesian inference. *The Annals of Statistics*, 38(3):1433–1459, 2010.

## A MCMC algorithm

The procedures to update each parameter in the MCMC algorithm are described below.

1. (Updating  $\omega_i(A)$ ) By Polson et al. (2013), the full conditional distribution of  $\omega_i(A)$  is

$$\text{PG}(n_i(A), \psi_i(A)).$$

2. (Updating  $\Lambda_{\cdot,k}$ ) The full-conditional posterior of  $\Lambda_{\cdot,k}$  is  $N(\mathbf{m}_{\Lambda,k}, \Sigma_{\Lambda,k})$ , where

$$\begin{aligned} \Sigma_{\Lambda,k}^{-1} &= \tau_k (I_M - \rho_k W^T) \Phi_k (I_M - \rho_k W) + \sum_{A \in \mathcal{N}(T)} \eta_k^2 \Omega(A), \\ \mathbf{m}_{\Lambda,k}^{-1} &= \sum_{A \in \mathcal{N}(T)} \eta_k \left[ \kappa(A) - \Omega(A) \left( \mu(A) \iota_M + \sum_{k'=1, k' \neq k}^K \eta_{k'}(A) \Lambda_{\cdot,k'} \right) \right]. \end{aligned}$$

3. (Updating  $\eta(A)$ ) The full-conditional posterior of  $\eta(A)$  is  $N(\mathbf{m}_{\eta(A)}, \Sigma_{\eta(A)})$ , where

$$\begin{aligned} \Sigma_{\eta(A)}^{-1} &= I_K + \Lambda^T \Omega(A) \Lambda, \\ \mathbf{m}_{\eta(A)} &= \Sigma_{\eta(A)} \Lambda^T [\kappa(A) - \mu(A) \Omega(A) \iota_M]. \end{aligned}$$

4. (Updating  $\phi_{i,k}$ ) The full conditional posterior of  $\phi_{i,k}$  is  $\text{Gamma}(a_{\phi,i,k}, b_{\phi,i,k})$ , where

$$a_{\phi,i,k} = \frac{\nu + 1}{2}, \quad b_{\phi,i,k} = \frac{1}{2} \left( \nu + \tau_k \tilde{\Lambda}_{i,k}^2 \right),$$

where  $\tilde{\Lambda}_{\cdot,k} = \{\tilde{\Lambda}_{i,k}\}_{i=1}^M = (I_k - \rho_k W) \Lambda_{\cdot,k}$ .

5. (Updating  $\tau_k$ ) We update  $\tau_k$  via  $\delta_1, \dots, \delta_K$  since  $\tau_k = \prod_{k'=1}^k \delta_{k'}$ . To this end, we define  $\tau_k^{(l)}$  for  $l \geq k$  as

$$\tau_k^{(l)} = \prod_{k'=1, k' \neq k}^l \delta_{k'}.$$

Then, the full conditional posterior of  $\delta_1$  is  $\text{Gamma}(a_{\delta,1}, b_{\delta,1})$ , where

$$\begin{aligned} a_{\delta,1} &= a_1 + \frac{MK}{2}, \\ b_{\delta,1} &= 1 + \frac{1}{2} \sum_{k'=1}^K \delta_{k'}^{(1)} \Lambda_{\cdot,k'}^T (I_M - \rho_{k'} W^T) \Phi_{k'} (I_M - \rho_{k'} W) \Lambda_{\cdot,k'}. \end{aligned}$$

Similarly, the full conditional posterior for  $\delta_k$  ( $k = 2, \dots, K$ ) is  $\text{Gamma}(a_{\delta,k}, b_{\delta,k})$ , where

$$\begin{aligned} a_{\delta,k} &= a_2 + \frac{M(K - k + 1)}{2}, \\ b_{\delta,k} &= 1 + \frac{1}{2} \sum_{k'=k}^K \delta_{k'}^{(k)} \Lambda_{\cdot,k'}^T (I_M - \rho_{k'} W^T) \Phi_{k'} (I_M - \rho_{k'} W) \Lambda_{\cdot,k'}. \end{aligned}$$

6. (Updating  $\rho_k$ ) The full conditional posterior of  $\rho_k$  is  $\text{Normal}_{(-\infty, \infty)}(m_{\rho, k}, s_{\rho, k}^2)$ , where

$$\begin{aligned} s_{\rho, k}^{-2} &= s_{\rho}^{-2} + \tau_k \mathbf{\Lambda}_{\cdot k}^T W^T \mathbf{\Phi}_k W \mathbf{\Lambda}_{\cdot k}, \\ m_{\rho, k} &= s_{\rho, k} [s_{\rho}^{-2} m_{\rho} + \tau_k \mathbf{\Lambda}_{\cdot k}^T W^T \mathbf{\Phi}_k \mathbf{\Lambda}_{\cdot k}]. \end{aligned}$$

## B Details of the numerical experiments

### B.1 Simulation settings in the illustration of the proposed tree embedding

We describe the simulation settings for the illustration provided in Section 2. We here combine the following two discrete distributions.

$$d_1 = (1/3, 1/3, 1/3), \quad d_2 = (1/2, 1/3, 1/6).$$

1. For the mixture model, for each  $i$  we simulate the distribution as

$$w_i d_1 + (1 - w_i) d_2,$$

where  $w_i$  is the mixture weight generated from the beta distribution  $\text{Beta}(0.25, 0.35)$ .

2. For the proposed model with the tree embedding, we consider the tree  $T$  that first split the set into the first category and the second and third categories, and then divide the latter categories. We simulate each distribution in the Euclidean space as

$$\lambda_{i1} \mathcal{E}_T(d_1) + \lambda_{i2} \mathcal{E}_T(d_2),$$

where  $\lambda_{i1}$  and  $\lambda_{i2}$  follow the standard normal distribution.

### B.2 Models considered in the application to the stay-population data

We describe the models compared to the proposed model in Section 3

1. Dirichlet Process Mixture Model(DPM)

$$\begin{aligned} \mathbf{Y}_i \mid \boldsymbol{\mu}_i &\sim \text{Multinomial}(N_i, \boldsymbol{\mu}_i), \quad i = 1, \dots, M, \\ \boldsymbol{\mu}_i \mid G &\sim G, \quad i = 1, \dots, M, \\ G \mid \alpha &\sim \text{DP}(\alpha, G_0), \\ \alpha &\sim \text{Gamma}(a, b), \\ G_0 &= \text{Dirichlet}(\boldsymbol{\eta}). \end{aligned}$$

In this framework,  $\mathbf{Y}_i$  denotes the vector of observed counts for the  $i$ -th observation, which follows a multinomial distribution with total count  $N_i$  and a latent probability vector  $\boldsymbol{\mu}_i$ . The

latent vectors  $\boldsymbol{\mu}_i$  are drawn from a random probability measure  $G$ , modeled as a Dirichlet Process. Here, the concentration parameter  $\alpha$  is assigned a Gamma prior to control the clustering sparsity, while the base measure  $G_0$  is specified as a symmetric Dirichlet distribution. We adopt this model as a benchmark because the DPM is widely recognized as a standard Bayesian nonparametric approach for clustering, allowing for flexible modeling of heterogeneity without fixing the number of clusters a priori. For posterior inference, we employ the Gibbs sampling algorithm described in Neal (2000) and Escobar and West (1995).

## 2. Log-normal model with Pair-wise difference prior (Log-normal PWD)

$$\begin{aligned}
\mathbf{Y}_i \mid \mathbf{u}_i &\sim \text{Multinomial}(n_i, \mathbf{p}(\mathbf{u}_i)), \quad i = 1, \dots, M, \\
p_{ij} &= F_{\text{LN}}(z_j; u_{i1}, e^{u_{i2}}) - F_{\text{LN}}(z_{j-1}; u_{i1}, e^{u_{i2}}), \quad j = 1, \dots, N, \\
&\pi(u_{11}, \dots, u_{M1}) \\
&\propto C(\tau_l, \lambda_l) \exp \left\{ -\frac{\tau_l}{2} \sum_{i=1}^M (u_{il} - \mu_l)^2 - \frac{\lambda_l}{2} \sum_{i < j}^M w_{ij} (u_{il} - u_{jl})^2 \right\}, \quad l = 1, 2, \\
\mu_l &\sim \mathcal{N}(0, a_\mu^{-1}), \quad \tau_l \sim \mathcal{G}(b_\tau, c_\tau), \quad \lambda_l \sim \mathcal{G}(b_\lambda, c_\lambda),
\end{aligned}$$

Sugasawa et al. (2020) proposed this formulation to estimate area-wise spatial income distributions from grouped data. In this model,  $\mathbf{Y}_i = (Y_{i1}, \dots, Y_{iN})^\top$  represents the vector of observed frequencies falling into  $N$  pre-defined intervals for the  $i$ -th area, where  $n_i = \sum_{j=1}^N Y_{ij}$  is the total sample size for the  $i$ -th area. The probability  $p_{ij}$  corresponds to the probability mass assigned to the  $j$ -th interval  $(z_{j-1}, z_j]$  by a latent Log-normal distribution with cumulative distribution function  $F_{\text{LN}}(\cdot)$ . Because the demographic data used in this study lacks observations for individuals under 15 years of age, we assume a left-truncated distribution. Specifically, the probability  $p_{ij}$  is formulated as a conditional probability given that the age is at least the lower bound  $z_0$ , which corresponds to 15 years. Consequently, the probability mass for each interval is normalized by  $1 - F_{\text{LN}}(z_0; u_{i1}, e^{u_{i2}})$  to ensure that the sum of probabilities across all observed intervals equals one.

The area-specific parameters are defined as  $\mathbf{u}_i = (u_{i1}, u_{i2})^\top$ , where  $u_{i1}$  denotes the mean and  $u_{i2}$  represents the log-transformed variance to ensure positivity. In the prior distribution for the area-wise parameters,  $\tau_l$  and  $\lambda_l$  act as precision parameters. The term  $C(\tau_l, \lambda_l)$  is the normalizing constant relevant to these precision parameters, defined as  $C(\tau_l, \lambda_l) = |Q(\tau_l, \lambda_l)|^{1/2}$  with  $Q(\tau_l, \lambda_l) = \tau_l I_M + \lambda_l W_*$ . Here,  $I_M$  is the  $M \times M$  identity matrix, and  $W_* = \text{diag}(w_1, \dots, w_M) - W$ , where  $w_i$  is the number of adjacent areas to area  $i$ , and  $W$  is an  $M \times M$  matrix with the  $(i, j)$ -th entry equal to  $w_{ij}$ . The adjacency weight  $w_{ij}$  is equal to one if area  $j$  is adjacent to area  $i$ , and zero otherwise. By introducing this latent stochastic structure where  $\lambda_l$  and adjacency weights  $w_{ij}$  shrink the differences between adjacent areas

toward zero, this model accounts for geographical dependencies, allowing it to borrow strength across neighboring areas and improve estimation accuracy for areas with small sample sizes. The details of the MCMC algorithm for posterior inference are provided in Sugasawa et al. (2020), and the corresponding R code is available at <https://github.com/sshonosuke/SPID>. However, to ensure convergence for the spatiotemporal population data, we slightly modified the original code by implementing an adaptive MCMC approach that tunes the step size of the Metropolis-Adjusted Langevin Algorithm during the burn-in period.